Pressure Sensitive Paint Application at Large Production Wind Tunnels

Yuichi SHIMBO[*], Keisuke ASAI[**]
National Aerospace Laboratory
7-44-1, Jindaiji-higashi, Mitaka, 182-8522, Japan

Nobuyoshi KOMATSU[***]
Mitsubishi Heavy Industries, Ltd.
10 Oye-cho, Minato-ku, Nagoya, 455-8515, Japan

Key words : Pressure sensitive paint, Wind tunnel, Pressure measurement

Abstract

A pressure sensitive paint (PSP) technique was established based on a commercially available paint and a CCD camera-based measurement system. To convert the paint data into pressure, a new PSP/TSP combined calibration was applied other than the conventional in situ calibration. The new method required no pressure tap to the model, and used a temperature sensitive paint (TSP) to compensate for the unfavorable temperature sensitivity of the PSP. It was first applied in the continuous 2m transonic wind tunnel testing where both pressure and temperature conditions on the model were steady, and the test results of a rigid-body axisymmetric model and a deformative wing-body model showed very good agreement with the pressure tap data. Then, the paint technique was expanded to the blowdown 1m supersonic wind tunnel testing where the model surface temperature changed with respect to time. The test results of a thin-wing SST model also showed good agreement with the pressure tap measurement even there was about 10K drop in the model surface temperature during 40 seconds blow at M=2. In addition, the paint data successfully provided valuable pressure field visualization through the work, which was not usually achieved by the conventional point measurement by the pressure taps.

* Currently Mitsubishi Heavy Industries, Ltd
   yuichi_shimbo@mx.nasw.mhi.co.jp
** asai@nal.go.jp
*** nobuyoshi_komatsu@mx.nasw.mhi.co.jp

1. Introduction

After the first development stage of a pressure sensitive paint (PSP) technique in early 1990's in the United States and Europe [1], it became popular because of its great advantages of a continuous pressure field measurement, and much lower cost and shorter time involved in model development and wind tunnel testing. However, these applications were mostly restricted to steady pressure measurements at continuous high-speed wind tunnels because the measurement accuracy was poor at low-speed regime where the pressure difference generated by the air flow was small, and the response of the PSP to rapid pressure change was too slow to be applied to unsteady pressure measurements. Furthermore, because the measurement principle of the PSP is based on chemical reactions, it usually has rather large temperature sensitivity, which leads to a measurement error due to non-uniform temperature distribution on the model surface or a temperature change between No-wind and On-wind conditions.

National Aerospace Laboratory (NAL) in Japan has been making effort since 1994 to develop its own paint formulations, to establish a test technique and to evaluate measurement accuracy. The present paper summarizes the continuous effort to expand the paint technique application to large production high-speed wind tunnels used in aircraft development, with a commercially available PSP and a CCD camera-based measurement system [2-4]. To solve the problem of the temperature sensitivity of the PSP, a new PSP/TSP combined calibration was

introduced and demonstrated in both transonic and blowdown supersonic testing. The transonic testing was conducted under the cooperative research program between NAL and Mitsubishi Heavy Industries, Ltd..

2. Measurement System

2.1 Paints

The PSP used in the present work was composed of a luminescent molecule, PtOEP (Platinum Octaethyl Porphyrin) and an oxygen permeable binder, GP-197. This paint was based on the well-known formulation developed by University of Washington [5] and was well examined at NAL [6]. The peak excitation wavelength was 366 nm in the UV region and the emission wavelength was 650 nm in red. The measurement principle of the temperature sensitive paint (TSP) is similar to the PSP and utilizes only the temperature sensitivity of the luminescent molecule, combined with an oxygen impermeable binder. The TSP used was composed of EuTTA (Europium thenoyltrifluoro-acetonate) and PMMA (polymethyl-methacrylate), which had the peak excitation wavelength of 350 nm and the emission wavelength was 612 nm [7].

2.2 Measurement System

Because the PSP and TSP described above had similar wavelength for excitation and emission light, both measurements were conducted with the same measurement system.

    The emission light from the paint layer was collected and quantified by a CCD camera-based measurement system constructed at NAL. The CCD camera was a water-cooled 14-bit camera and the image size was 1008 x 1018 pixels. Optical filters were attached to the camera lens to collect only emission light from the paint layer.

    A xenon lamp was used as an excitation light source and the light was introduced through optical fibers to light reflectors. Each light reflector had an optical filter so that only

the UV light for paint excitation went through.

2.3 Sample Test

The photophysical characteristics of each paint was evaluated in the static calibration chamber based on the same measurement system described above [8]. The sample tests were conducted with sample plates coated with the same batch of the paint as one applied to the model. Figures 1 show typical results of the sample test both for the PSP and TSP. Each line corresponds to the variation of the luminescence ratio at a constant surface temperature, where the reference condition was set to pressure Pc and temperature Tc. The PSP data show high pressure sensitivity from near vacuum to 100 kPa, however, its temperature sensitivity is also strong. On the other hand, the TSP data show high temperature sensitivity with slight pressure sensitivity. For a later use, the sample test data were fitted to polynomial curves in the form of eqs. (1) and (2).

$$\text{PSP} \qquad \frac{Ip(Pc,Tc)}{Ip(P,T)} = \sum_{i=0}^{4} Api(T)\left(\frac{P}{Pc}\right)^i \qquad (1)$$

$$\text{TSP} \qquad \frac{It(P,T)}{It(Pc,Tc)} = \sum_{i=0}^{3} Ati(P)\left(\frac{T}{Tc}\right)^i \qquad (2)$$
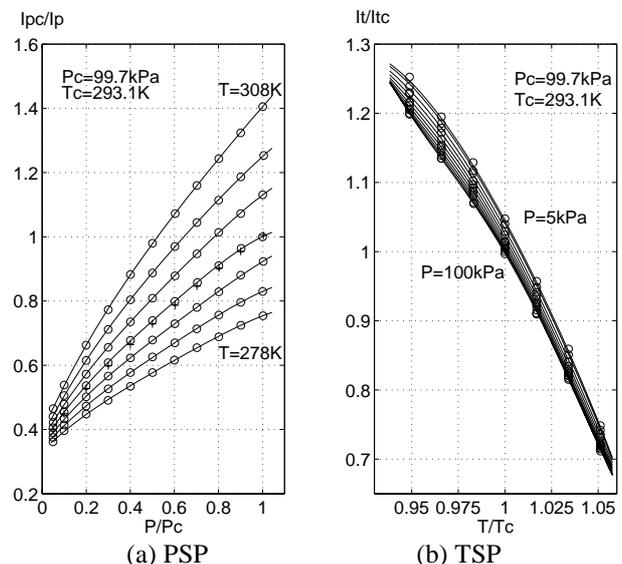

Figure 1 Typical sample test results of the paints

Here, Ip and It indicate the emission light intensity of the PSP and TSP, respectively.

3. Data Reduction

In the wind tunnel testing, No-wind images were captured as reference images prior to the On-wind image acquisition under the same exposure condition. The Dark images were also captured with the mechanical shutter of the CCD camera closed so that no light came into the CCD array.

The data reduction of these images was carried out in the sequence shown in Figure 2, and it was almost automated using Matlab software on a personal computer.

At first, all three-type images were averaged to minimize a measurement error due to a single-shot photon noise of the CCD camera, and then the averaged dark image was subtracted from the averaged No-wind and On-wind image as initial output correction.

Second, the luminescence ratio of the emission light from the paint layer between No-wind and On-wind conditions were computed. Theoretically, any non-uniformity of the paint layer thickness and the excitation light intensity was canceled out by this nondimensionalization. In this process, a two-dimensional registration was applied to make correction for the model displacement and deformation between the No-wind and On-wind conditions. A three-dimensional registration was also applied to relate the three-dimensional model geometry to two-dimensional image so that the pressure data at an arbitrary point could be picked up from the image. Several target markers were put on the model surface to be used in these registrations.

Finally, the luminescence ratio data were converted into pressure data through two paint calibration methods, a conventional in situ calibration and a new PSP/TSP calibration.

The in situ calibration uses pressure tap data obtained under the same flow condition as the paint measurement. The relation between the pressure tap data and the luminescence ratio data at corresponding locations is represented by
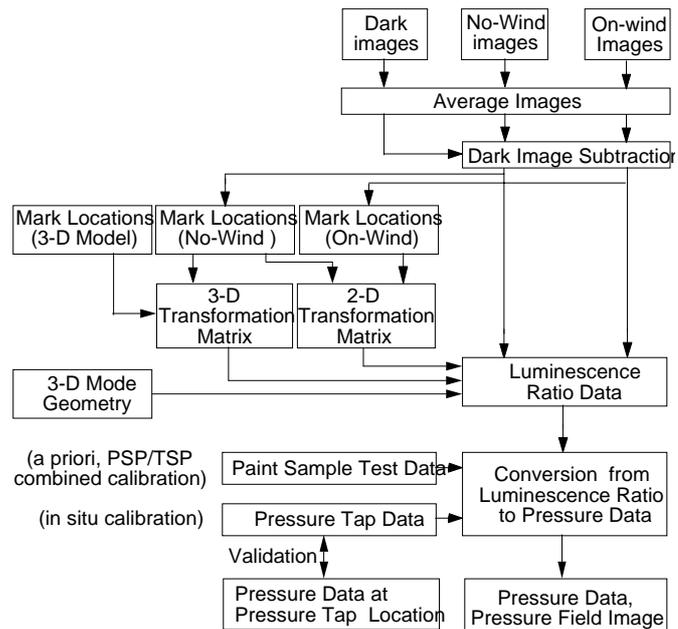

Figure 2 Flowchart of the data reduction

a polynomial fitting in the form of eq. (3).

$$\frac{Ip(Pr, Tr)}{Ip(P, T)} = \sum_{i=0}^{4} Ci\left(\frac{P}{Pc}\right)^i \tag{3}$$

Here, Pr and Tr indicate the pressure and temperature in the reference No-wind condition. Then, the polynomial fitting is applied to all other portion of the model to determine the pressure. The advantage of the in situ calibration is that the effect of the temperature difference between the No-wind and On-wind conditions are automatically included in the polynomial fitting. However, at least several pressure taps are necessary on the model, and they should be properly located so that all the pressure and temperature range on the painted surface are covered by the pressure tap information.

The PSP/TSP combined calibration, on the other hand, uses TSP to measure the temperature distribution on the model surface to compensate for the unfavorable temperature sensitivity of the PSP. For an arbitrary point on the model, if luminescence ratio of both PSP and TSP and the static sample test data in the form of eqs. (1) and (2) are available, the pressure, P, and model surface temperature, T,

in the On-wind condition are two unknowns in the following two equations.

$$\text{PSP} \quad \frac{Ip(Pr,Tr)}{Ip(P,T)} = \frac{Ip(Pr,Tr)}{Ip(Pc,Tc)} \Big/ \frac{Ip(P,T)}{Ip(Pc,Tc)} \qquad (4)$$

$$\text{TSP} \quad \frac{It(P,T)}{It(Pr,Tr)} = \frac{It(P,T)}{It(Pc,Tc)} \Big/ \frac{It(Pr,Tr)}{It(Pc,Tc)} \qquad (5)$$

These are solved by iteration assuming the thermal conditions of the PSP and TSP layer on that point are same. The No-wind pressure, Pr, is represented by the ambient pressure of the test section and No-wind temperature of the paint surface, Tr, is represented by one measured on the model surface when the model surface temperature is uniform. The biggest advantage of this method is that no pressure tap is required to the model and it leads to great potential to revive an existing force model without any pressure taps for pressure measurement.

4. Applications

4.1 Rigid-body (H-II) model in Transonic Testing

This experiment was the first application of the PSP technique to a large production wind tunnel, and the main objective was to make a detailed evaluation of the measurement accuracy. A rigid axisymmetric body model was used to demonstrate the paint technique application to a highly curved surface, and to avoid a measurement error due to the elastic model deformation.

A schematic of the experiment is shown in Figure 3. The experiment was conducted at the continuous-type 2m Transonic Wind Tunnel at NAL. The model was a 4.3% scale model of a nose fairing part of the Japanese H-II launcher and was completely axisymmetric. The model was equipped with 91 pressure taps arranged on a meridian and five more on the opposite side for a conventional static pressure measurement. The model was attached directly to the sting support system of the tunnel without a balance.
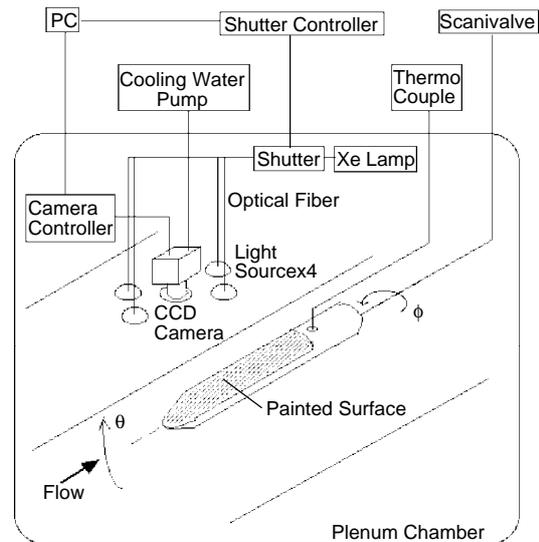

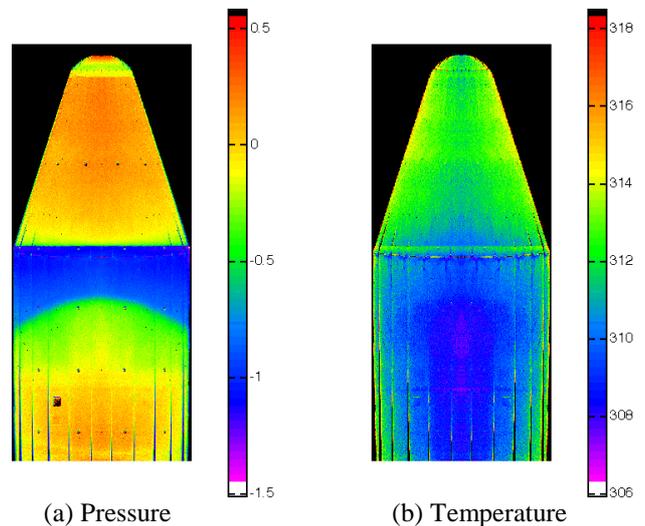Figure 3 Experimental set-up for the H-II test

(a) Pressure   (b) Temperature

Figure 4 Pressure and temperature field for the H-II test (M=0.9, α=4 deg)
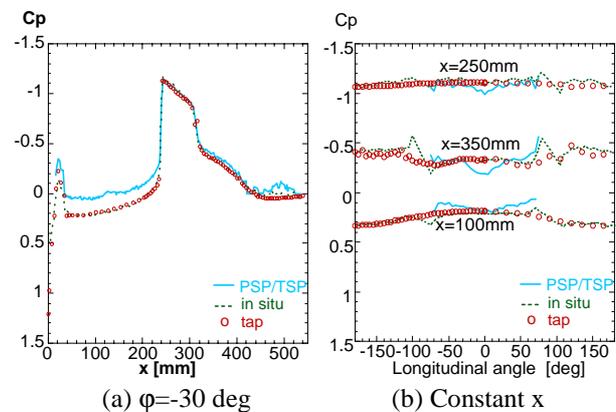

(a) φ=-30 deg   (b) Constant x

Figure 5 Comparison between the PSP and pressure tap measurements for the H-II test (M=0.9, α=4 deg, φ=0 deg corresponds to upper centerline and x=0 corresponds to the nose tip of the model)

The PSP was airbrushed on the white optical undercoat applied on the upper surface of the model, over the five pressure taps. The TSP, on the other hand, was airbrushed on a narrow strip of an adhesive Mylar film and attached on the opposite side of the PSP layer. A sheet-type thermocouple was directly attached to the model behind the PSP layer to measure a typical temperature on the model surface. Both the CCD camera and the excitation light reflectors were put on the ceiling of the test section.

The uniform flow condition was set to M=0.9, and the PSP measurement was conducted at five pitch angles (θ=0, ±4 and ±8 deg), where θ=–4 and –8 deg corresponded to the lower surface measurements at α=4 and 8 deg, respectively. The TSP tape was applied after all the PSP measurements were completed and only the upper surface was investigated. A holding time for one to two minutes were kept after the angle of attack was changed so that the thermal condition of the paint layer was in an equilibrium condition. In addition, pressure tap measurements were conducted at every 5 or 15 roll angle at each angle of attack to collect detailed pressure tap data both in the streamwise and circumferential directions.

Figures 4 show a pressure and temperature field on the whole upper surface at α=4 deg computed using the PSP/TSP combined calibration. The pressure image captures a small expansion region near the nose tip, rapid expansion at the nose/cylinder junction and a round-shape shock wave followed by a separation region with a gradual pressure recovery. The temperature filed shows higher temperature at the nose part and a considerable temperature distribution on the model surface.

Figures 5 show comparisons between PSP and pressure tap measurements along a meridian at -30 deg longitudinal angle, and at three constant streamwise stations, x=100 mm (nose part), 250 mm (just behind the nose/cylinder joint) and 350 mm (cylinder part). For the PSP data converted by the in situ calibration using the five pressure tap information on the PSP

layer, the agreement with the pressure tap data are very good both in high and low pressure regions except around φ=±90 deg where the view angle of the camera was very shallow and the paint image was blurred near the model edge. The PSP data converted by the PSP/TSP combined calibration also agree well on the cylinder part even no pressure tap data were used in the data reduction. They were slightly worse than one by the in situ calibration on the nose part, probably because the total temperature of the tunnel were different between the PSP and TSP measurements, and the thermal condition of the PSP layer on the white paint and the TSP layer on the Mylar film were different in this experiment.

4.1.2 Deformative Wing-Body (MU-300) Model in Transonic Testing

After the rigid-body model experiment, another experiment was conducted with a business jet model. The main objectives were to expand the paint technique to a deformative model and to demonstrate the PSP/TSP combined calibration in general transonic testing.

Figure 6 illustrates the schematic of the experiment. The experiment was also conducted at NAL 2m transonic wind tunnel. The model was an 8% scale model of the MU-300 business jet in the complete aircraft
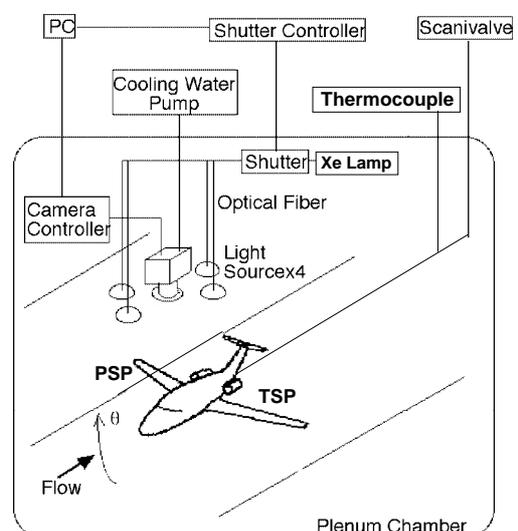

Figure 6 Experimental set-up for the MU-300 test

configuration. The model was equipped with 32 pressure taps arranged on four rows of the upper surface of the starboard wing. In this experiment, the PSP was applied only on the upper surface of the starboard wing and the TSP was applied on another wing. The emission light from both paints was captured in the same image by the CCD camera put on the ceiling of the test section. An inclinometer was installed inside the model to measure the angle of attack and a sheet-type thermocouple was directly attached to a rear part of the wing lower surface to measure the reference No-wind temperature of the model surface. The test condition was set to M=0.6~0.8, and α=0~4.6 deg with no sideslip

angle.

Figures 7 show two typical pressure fields computed by the PSP/TSP combined calibration. A clear shock wave exists on the wing, and the forward displacement of the shock wave near the wing tip and slightly higher pressure on the inner wing region in front of the nacelle are also visualized. With increasing the Mach number and the angle of attack, the shock wave became strong and its location moved aftward.

Figures 8 show the comparison between the PSP and pressure tap measurements. Both PSP data computed by the PSP/TSP combined calibration and the in situ calibration show
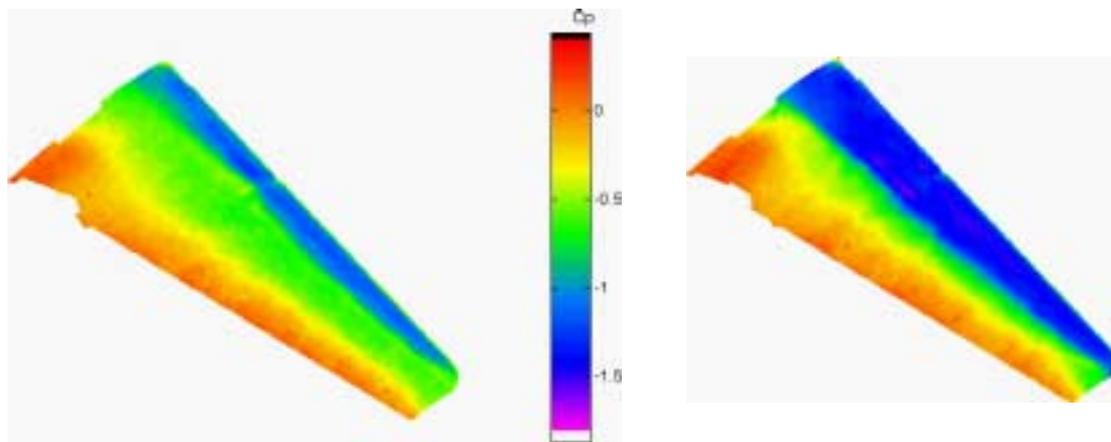
(a) M=0.73, α=2.3deg   (b) M=0.75, α=4.7 deg

Figure 7 Typical pressure fields for the MU-300 test

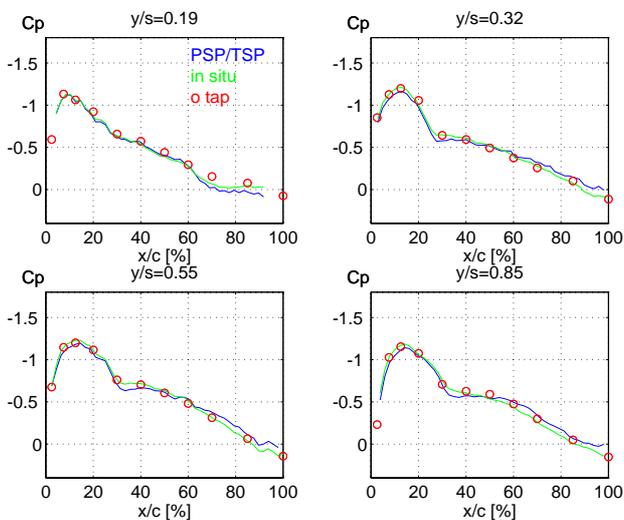

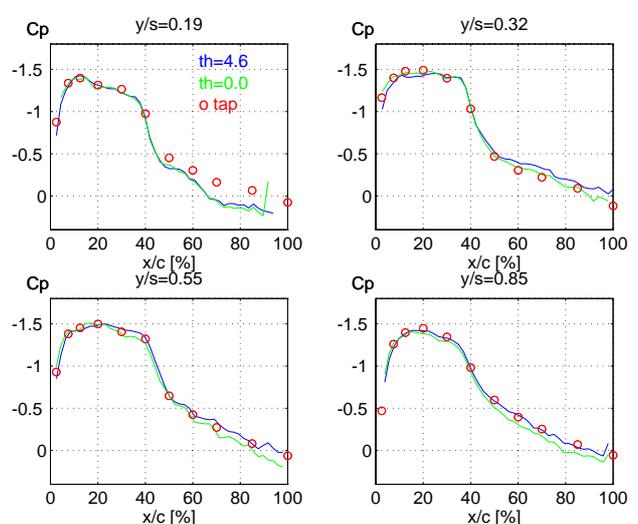Figure 8 Comparison between PSP and pressure tap measurements for the MU-300 test (M=0.73, α=2.3deg)

Figure 9 Evaluation of the two-dimensional registration for the wing deformation in the MU-300 test (M=0.75, α=4.7deg)

similar good agreement with the pressure tap data, which indicates the PSP/TSP combined calibration worked as well as the in situ calibration without using any pressure tap information.

To evaluate the performance of the two-dimensional registration to correct the model displacement and deformation between the No-wind and On-wind conditions, the same On-wind image taken at M=0.75 and α=4.7 deg was combined with two No-wind images taken at pitch angle θ=0 and 4.6 deg for the data reduction by the PSP/TSP combined calibration. Figures 9 show the resulting pressure distributions and both PSP data show very good agreement with the pressure tap data even there was about five degrees difference in the No-wind pitch angle. This indicates the No-wind image is not necessary for every On-wind condition, which reduces the time for No-wind image acquisition.

4.3 Blowdown Supersonic Testing of an SST Model

A pressure measurement of an SST model in supersonic wind tunnel testing is one of the best applications of the paint technique, because the pressure field is usually very complex due to the engine/airframe interactions although only restricted number of conventional pressure taps are usually available for a scaled wind tunnel model of the thin-wing SST configuration. However, this is also a new challenge for the PSP/TSP combined calibration because wind tunnel testing of SST models are mainly conducted at blowdown supersonic wind tunnels, where the surface temperature of the model changes at every moment whereas the pressure is held constant.

A schematic of the experimental set-up is shown in Figure 10. The experiment was conducted in the blowdown-type 1m Supersonic Wind Tunnel at NAL. The test section is one meter square and a typical run time is up to about 40 seconds. NAL is promoting the National Experimental Supersonic Transport

(NEXST) Program since 1996 [9] and the model was an 8.5% scale pressure model of one of the candidate configurations. The model had 90 pressure taps arranged both on the body and wing, and sting supported without a balance. To evaluate the effect of propulsion system installation, two types of flow-through nacelles (large and small) were prepared to be attached at η=0.3 (30% semispan location) of the wing lower surface via diverters.

In this experiment the PSP was applied on both upper and lower surface of the portside wing and lower half of each portside nacelle, and the TSP was applied on another side. The model was set to 0 deg in pitch and ±90 deg in
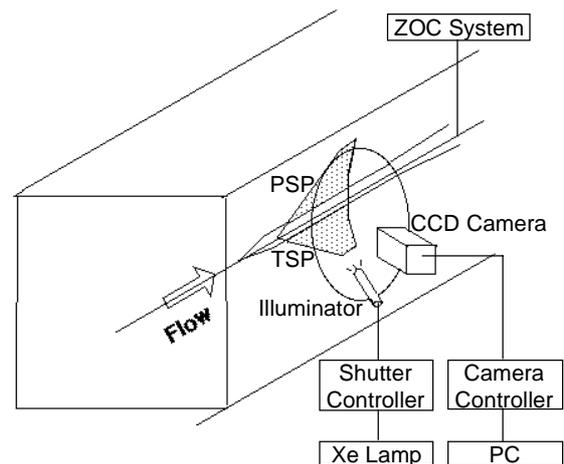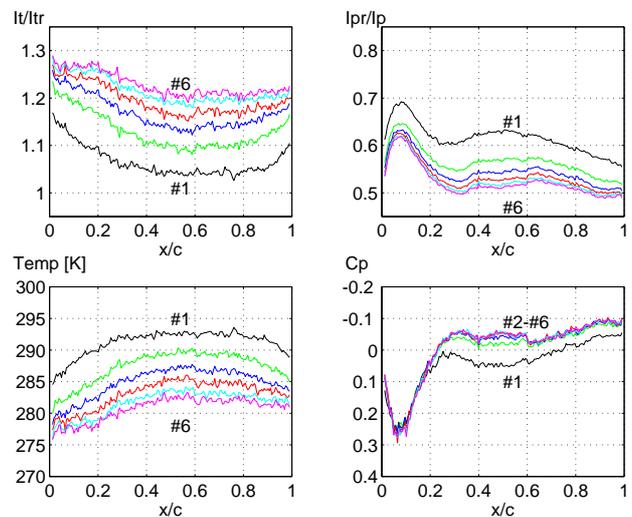

Figure 10 Experimental set-up for the SST test

Figure 11 Demonstration of the PSP/TSP combined calibration for the SST test (M=2, η=0.5, Large nacelle configuration)

roll so that either upper or lower wing surface was visible through one of the schlieren windows of the tunnel. Another side of the schlieren window was covered with a dark curtain and both the CCD camera and the illuminating light system were set inside a simple dark room.

The experiment was conducted only at 0 deg angle of attack with no sideslip, and the uniform flow Mach number was set to M=1.4, 1.6, 1.8 and 2.0. The experiment was composed of four parts; upper and lower surface measurements of the clean configuration, lower surface measurements with small nacelles and with large nacelles. The conventional pressure tap measurement was conducted by an electric pressure scanning system simultaneously with the image acquisition.

In each blow of the tunnel, the first On-wind image was captured about three seconds after the uniform flow of the tunnel was established because the typical response time to a rapid pressure change of the PSP used in this experiment was reported to be about two seconds [10]. Then, five more images were captured during the 40 seconds blow. No averaging was applied to the On-wind images in the data reduction because the thermal condition

of the paint layer was different from one image to another. No-wind images were taken in advance after the model was left in an ambient condition for a long time and averaged image was used for the data reduction.

Figures 11 show sample results for the large nacelle configuration at M=2, along η=0.5 where the maximum wing thickness is 4.9 mm. The luminescence ratio data of the TSP in Figure 11(a) increase and the luminescence ratio data of the PSP in Figure 11(b) decrease with respect to time. As a result of applying the PSP/TSP combined calibration, the corresponding temperature data in Figure 11(c) indicate the model surface temperature dropped about 10K from #1 to #6 measurement. The corresponding pressure distribution in Figure 11(d) show higher pressure at the #1 measurement, however, later the pressure distributions of the #2 to #6 measurements agreed well even though there was a large temperature change. These results indicate the PSP/TSP combined calibration successfully corrected the temperature sensitivity of the PSP, and it was also found that waiting time about 10 to 15 seconds after the uniform flow was established (#2 and #3 measurements) was enough for the paint measurement in this
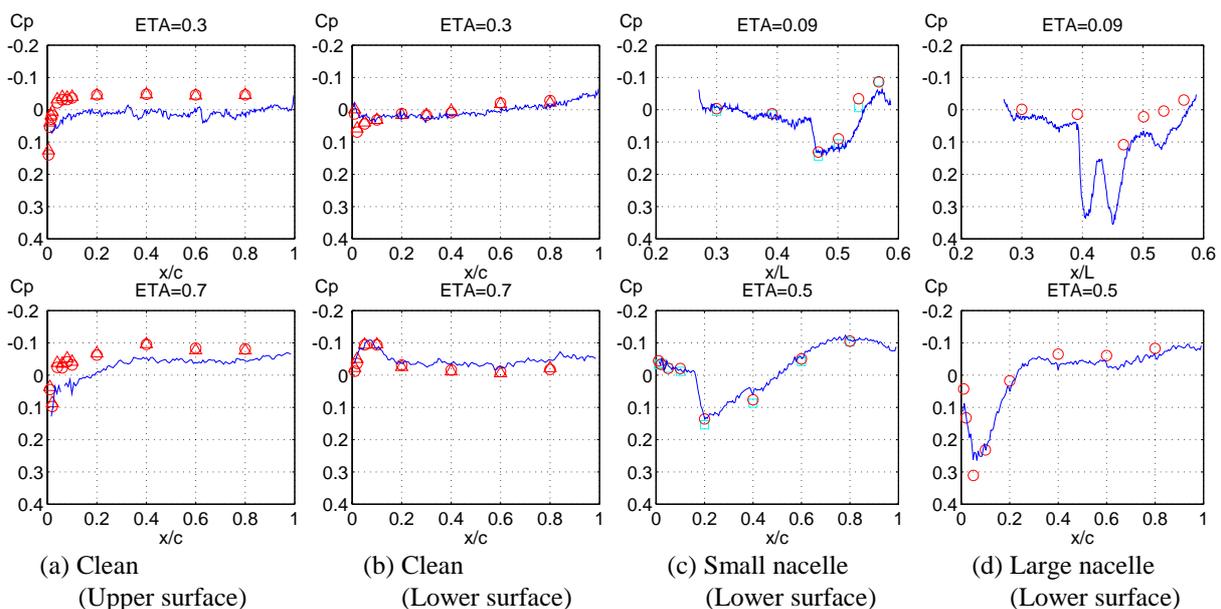

(a) Clean
(Upper surface)

(b) Clean
(Lower surface)

(c) Small nacelle
(Lower surface)

(d) Large nacelle
(Lower surface)

Figure 12 Comparison between the PSP and pressure tap measurements for the SST test (M=2, Solid lines indicate the PSP measurement and circles indicate pressure tap data)

particular blowdown supersonic tunnel application. The first measurement (#1) showed poor agreement probably because the thermal condition of the paint surface changed rapidly and was not same for one wing with PSP to another with TSP right after the uniform flow was established.

Figures 12 show comparisons between the #3 measurement of the PSP data and the pressure tap data at M=2 for all four configurations. Although the upper surface measurement of the clean configuration show a certain shift toward a higher pressure (positive Cp) direction, the other three lower surface measurements show very good agreement with the pressure tap data. For the small and large nacelle configurations, the pressure distributions show rapid changes due to the shock waves generated by the nacelle and diverter described later, which was not depicted by the discrete pressure tap measurement.

Figure 13(a) shows the relation between the PSP data and the pressure tap data for 411 samples in total at every Mach number and configuration. The agreement is good at the pressure range from 20 to 60 kPa and the PSP test technique with the PSP/TSP combined calibration is found to be feasible even in the blowdown tunnel application. Figure 13(b) shows statistical analysis of the data in Figure 13(a). The mean value of the difference between the PSP data and the pressure tap data was 3.18 kPa, which corresponds to about 3% of the atmospheric pressure and the standard deviation was 2.81 kPa.

Finally, Figures 14 show the whole pressure field of the lower surface of both small and large nacelle configurations at M=2.0. For the small nacelle configuration, there is a round-shaped strong compression region generate by the shock wave in front of the nacelle inlet. Another compression region is expanding in both inner and outer wing directions from the front edge of the diverter (not visible in the image), followed by a suction region coming from the converging aft part of the diverter. For the large nacelle configuration, the shock pattern
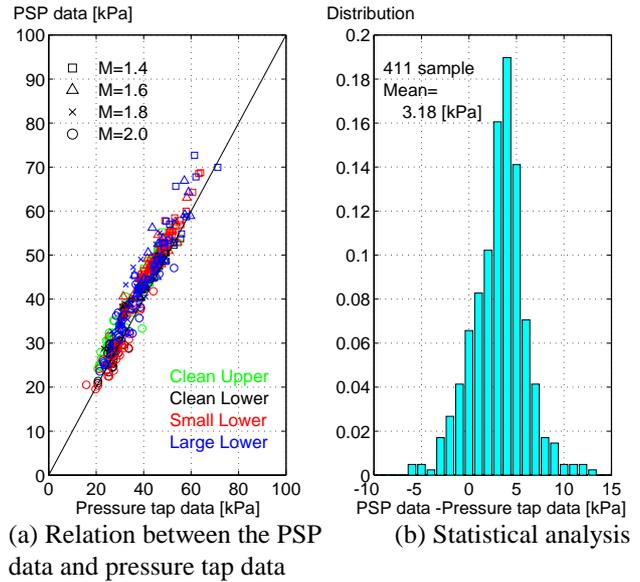

(a) Relation between the PSP data and pressure tap data
(b) Statistical analysis

Figure 13 Measurement accuracy for the SST test

(a) Small nacelle
(b) Large nacelle
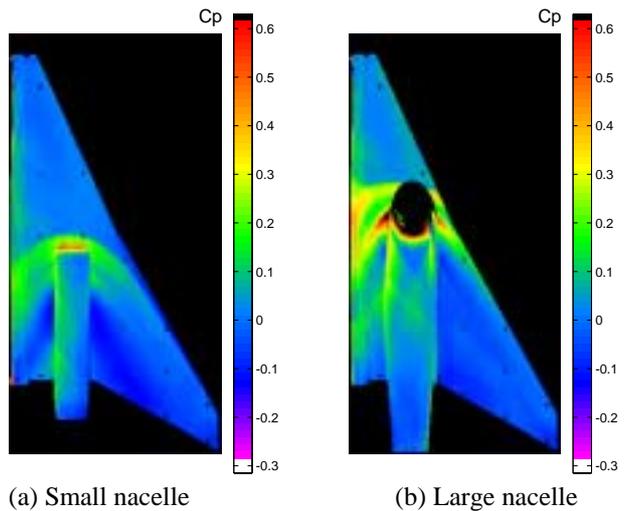
Figure 14 Pressure field for the SST test (M=2)

is more complex. There is a compression region in front of the nacelle inlet and it expands beyond the leading edge, which indicates the effect of the nacelle installation expanded to the upper surface. There is another pair of shock waves originating from the front edge of the diverter and their three-dimensional traces are also visible on the nacelle lower surface as boundaries of the triangular low pressure region. An additional higher pressure region is visible at the inner mid part of the nacelle, which is assumed to be coming from another side of the wing.

5. Conclusions

The pressure sensitive paint (PSP) technique was established and demonstrated in the large production wind tunnels in Japan. The PSP data converted by the new PSP/TSP combined calibration showed good agreement with the pressure tap measurement, and worked as well as the conventional in situ calibration without using any pressure tap information in the transonic testing. The method successfully corrected the unfavorable temperature sensitivity of the PSP and expanded the paint technique application to blowdown supersonic testing where the model surface temperature changed time by time. In addition, the paint data successfully provided valuable pressure field visualization through the work, which was not usually achieved by the point measurement by the pressure taps.

Besides using the PSP as an ordinary test technique for a steady pressure measurement in high-speed wind tunnels, further improvement is necessary to expand it to low-speed wind tunnel testing, unsteady pressure measurements and any other non-aerospace applications. The development of new measurement system is for the wind tunnel side, and the development of new paint formulation with less temperature sensitivity, high pressure sensitivity and faster response time is for the chemical side.

Acknowledgment

References

[1] Crites R. C., "Measurement Techniques -PRESSURE SENSITIVE PAINT TECHNIQUE", von Karman Institute for Fluid Dynamics, Lecture series 1993-05

[2] Shimbo Y., Asai K., Kanda H., Iijima Y., Komatsu N., Kita S. and Ishiguro M., Evaluation of Several Calibration Techniques of Pressure Sensitive Paint at Transonic Testing, AIAA-98-2502

[3] Shimbo Y., Asai K., Kanda H., Iijima Y., H. Sugiura, Komatsu N., Kita S. and Ishiguro M., Pressure Sensitive Paint Application to a Business Jet Model in Transonic Testing, 7th Pressure Sensitive Paint Workshop, West Lafayette, Oct., 1999

[4] Shimbo Y., Noguchi M., Iijima Y. and Asai K., Blowdown Tunnel Application of Pressure Sensitive Paint, AIAA-99-3169

[5] McLachlan B. G., Kavandi J. L., Callis J. B., Gouterman M., Green E., Khalil G. and Burns D., "Surface pressure field mapping using luminescent coatings", Experiments in Fluids 14 (1993)

[6] Asai K., Kanda H., and Iijima Y., "Luminescence Characteristics of Pressure Sensitive Paint Based on Platinum Octaethylporphyrin", Proc. of the 23rd Symposium on Visualization, J. of Flow Vis. Soc. of Japan, Vol. 15, Suppl. No. 1, 1995 (in Japanese).

[7] Liu T., Campbell B. T., Burns S. P. and Sullivan J. P., "Temperature and Pressure-Sensitive Luminescent paints in Aerodynamics", Apl. Mech. Rev., Vol. 50, No. 4, 1997

[8] Asai K., Kanda H., Iijima Y., Lee S. and Okura I., "Sample Tests of Pressure-Sensitive Paints with 49 Different Formulations", Proc. of the 25th Symposium on Visualization, J. of Flow Vis. Soc. of Japan, Vol. 17, Suppl. No. 1, 1997 (in Japanese).

[9] Yoshida K., Overview of NAL's Program Including the Aerodynamic Design of the Scaled Supersonic Experimental Airplane, RTO-EN-4, Nov. 1998

[10] Baron A. E., Danielson J. D. S., Gouterman M., Wan J. R., Callis J. B. and McLachlan B., "Submillisecond response times of oxygen-quenched luminescent coatings", Rev. Sci. Instrum. 64 (12), Dec. 1993, pp. 3394-3402